

TEXTMASTERO: MASTERING HIGH-QUALITY SCENE TEXT EDITING IN DIVERSE LANGUAGES AND STYLES

Tong Wang, Xiaochao Qu, and Ting Liu
MT Lab

ABSTRACT

Scene text editing aims to modify texts on images while maintaining the style of newly generated text similar to the original. Given an image, a target area, and target text, the task produces an output image with the target text in the selected area, replacing the original. This task has been studied extensively, with initial success using Generative Adversarial Networks (GANs) to balance text fidelity and style similarity. However, GAN-based methods struggled with complex backgrounds or text styles. Recent works leverage diffusion models, showing improved results, yet still face challenges, especially with non-Latin languages like CJK characters (Chinese, Japanese, Korean) that have complex glyphs, often producing inaccurate or unrecognizable characters. To address these issues, we present *TextMastero* - a carefully designed multilingual scene text editing architecture based on latent diffusion models (LDMs). *TextMastero* introduces two key modules: a glyph conditioning module for fine-grained content control in generating accurate texts, and a latent guidance module for providing comprehensive style information to ensure similarity before and after editing. Both qualitative and quantitative experiments demonstrate that our method surpasses all known existing works in text fidelity and style similarity.

1 Introduction

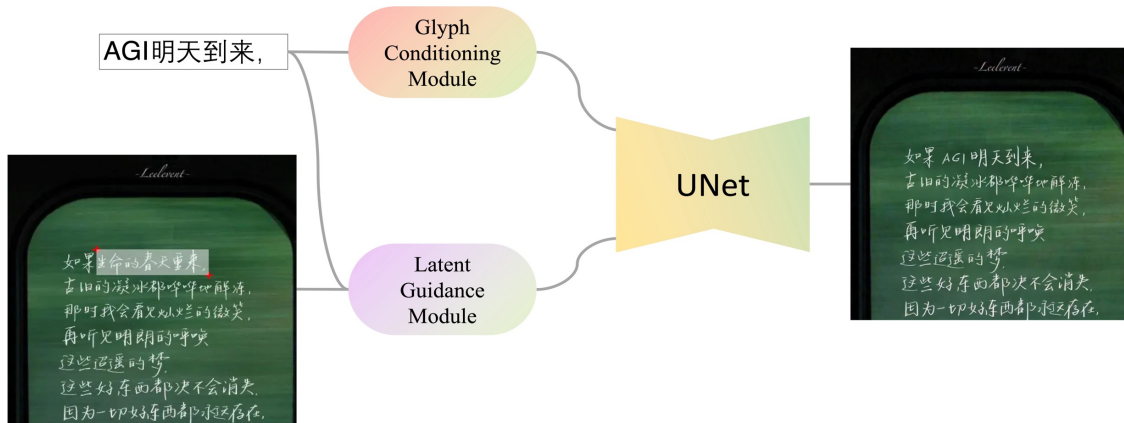


Figure 1: Overall Architecture

Scene text editing, a sub-field of general image editing, is a challenging task that aims to modify text in images while preserving the original style and maintaining visual coherence. It has significant applications for both regular users and professional designers, especially for those typefaces that are hard to find or even unable to be defined. Despite recent advancements, achieving high-quality results across diverse languages and complex visual scenarios remains a formidable challenge, particularly for non-Latin scripts with intricate glyph structures.

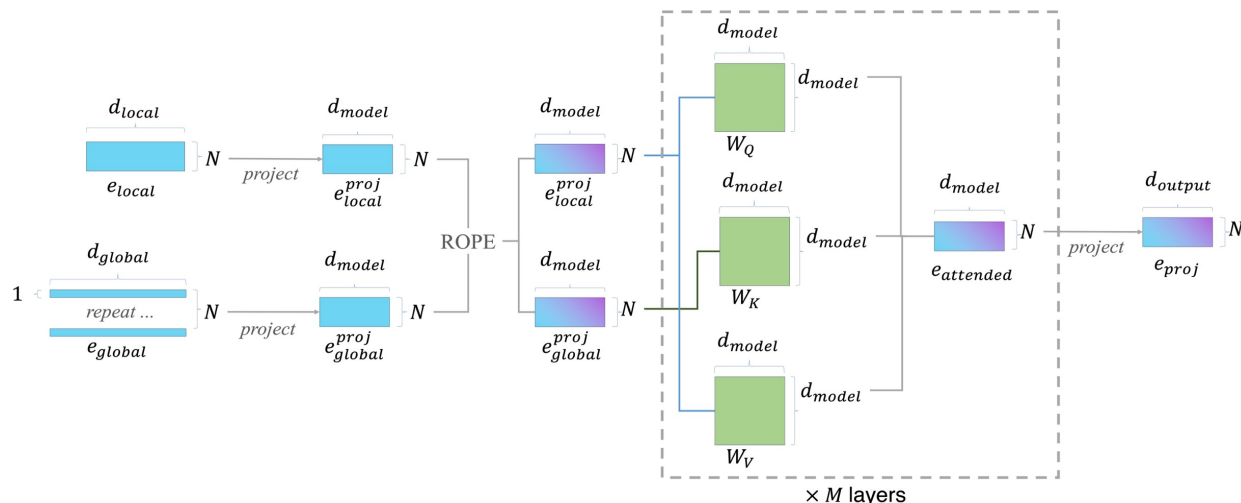


Figure 3: Glyph Transformer

- We propose a style encoder to encode the text region as additional style guidance for the UNet for better style coherency

Our contributions can be summarized into two modules: Glyph Conditioning Module and Latent Guidance Module (see Section 3 for details). Ablation studies has also shown effectiveness and necessity for each of our design.

2 Related Work

2.1 Scene Text Editing

Scene text editing has been approached through two main paradigms: GAN-based Lee et al. [2021], Wu et al. [2019], Roy et al. [2020], Qu et al. [2023] and diffusion-based Ji et al. [2023], Chen et al. [2023a], Tuo et al. [2024]. GAN-based works, such as STEFANN Roy et al. [2020], utilize style transfer concepts by employing a font-adaptive model to preserve text structures and another to extract and transfer style information.

Diffusion-based models employ two primary conditioning mechanisms: cross-attention guidance and direct latent space guidance. For cross-attention, AnyText Tuo et al. [2023] uses a pretrained OCR model to extract features from a rendered glyph image, incorporating these alongside image descriptions encoded by CLIP model’s text branch. DiffUTE replaces CLIP guidance with fixed-length features from TrOCR’s Li et al. [2023] last hidden state. DiffSTE Ji et al. [2023] proposes a dual cross-attention mechanism using CLIP embeddings and a character encoder. Our work utilizes the same pretrained OCR model as AnyText but introduces character-level fine-grained features with various techniques (detailed in section 3.1).

Direct latent space guidance, exemplified by ControlNet Zhang et al. [2023], encodes input conditions via convolution layers and adds them to original latents. However, this approach tends to align the generated image with the condition’s geometry, which is undesirable for scene text editing as we only want to encode style of the text region, not geometry contents in it. Thus, following Tuo et al. [2023], we provide latent conditions in an indirect way by concatenating latent style features to original UNet’s input convolution feature map, followed by another convolution layer to project back to UNet’s original dimension.

2.2 Diffusion Models

Diffusion models in deep learning were inspired by non-equilibrium thermodynamics. The forward pass destroys data by adding noise iteratively with some schedule, while the backward pass, which is the learning process, tries to restore the data. After training, we get a generative model since we can start from noise to generate new data samples. DDPM Ho et al. [2020] is the first work that used diffusion models for image generation and has become the foundation of most of today’s diffusion models. Since its introduction, diffusion models for image generation have diverged into two directions: pixel space denoising models such as Imagen Saharia et al. [2022], and latent space models (LDMs) Rombach et al. [2022] that firstly encode images to latent space, denoise the latents, then decode them back to image

space. The latter is less computationally intensive, hence it is more popular than the former for downstream tasks. Our work is based on a pretrained text-to-image LDM model. The training objective of LDMs can be written as:

$$L_{\text{LDM}} := \mathbb{E}_{\mathcal{E}(x), c, \epsilon \sim \mathcal{N}(0,1), t} \left[\|\epsilon - \epsilon_{\theta}(z_t, c, t)\|_2^2 \right].$$

\mathcal{E} is the encoder that compresses x to get latents z . ϵ represents the ground truth noise that was added to z in the forward pass. ϵ_{θ} is the time-dependent model that predicts the noise added given time step t , realized by a UNet Ronneberger et al. [2015]. c is the extra condition that guides the denoising process. Once the denoising process is finished, we decode the latents with $\hat{x} = \mathcal{D}(\hat{z})$ to get the resulting image. Our work can be summarized as designing novel glyph conditions c and additional style guidance that operates on latents z_t .

2.3 Feature Fusion

Feature fusion is a common technique in computer vision to combine complementary information from different sources or representations. Early approaches like skip connections He et al. [2016] and Feature Pyramid Networks Lin et al. [2017] demonstrated significant performance improvements by combining features between different layers and scales of the network. Recent works stress the same thing. Jiang et al. [2024] analyzed feature maps of CLIP Radford et al. [2021] and DINOv2 Oquab et al. [2023] in detail and found that the intermediate representations of different layers have distinct characteristics. For example, attention maps of CLIP show that shallow layers focus on local features while the deep layers focus on global ones. This suggests that not only is feature fusion useful in convolutional networks, but also in transformer-based vision models, encompassing most commonly used neural networks today. Thus, we propose two types of feature fusion to fully utilize the OCR recognition model’s capability. We fuse backbone features with a FPN-like fusion module and combine backbone and neck features with our proposed Glyph Transformer. See section 3.1 for details.

3 Method

Figure 1 presents the overall architecture of our proposed approach, which builds upon the latent diffusion models introduced by Rombach et al. [2022]. For clarity, we have omitted the VAE in this figure, but it is included in Figure 2. Our framework introduces two key modules tailored for scene text editing: a glyph guidance module that conditions text content, and a latent guidance module that handles text position and style conditions. These modules work together to enhance the model’s ability to edit scene text while preserving the desired content, position, and style characteristics.

3.1 Glyph Conditioning Module

Unlike text-to-image LDMs that primarily use CLIP Radford et al. [2021] for conditioning, we remove CLIP guidance as it’s not ideal for scene text editing. Instead, following Tuo et al. [2023], we incorporate the pretrained PaddleOCR-v4 recognition model PaddlePaddle [2023] for encoding input texts. We introduce more fine-grained controls by leveraging the OCR model’s capabilities. As shown in Figure 2 (up), given a text input x , we render it to $x_{\text{local}} \in \mathbb{R}^{N \times 36 \times 48}$, a series of single-character glyph images, and $x_{\text{global}} \in \mathbb{R}^{48 \times 320}$, a full text line glyph image. These are fed into the OCR model, yielding backbone and neck features:

$$F_{OCR}(x_{\text{local}}) = (e_{\text{backbone}}^{\text{local}}, e_{\text{neck}}^{\text{local}})$$

$$F_{OCR}(x_{\text{global}}) = (e_{\text{backbone}}^{\text{global}}, e_{\text{neck}}^{\text{global}})$$

We then use two glyph transformers to capture interactions between local and global features for both backbone and neck modules. Finally, an aggregator A projects and concatenates backbone $e_{\text{backbone}} \in \mathbb{R}^{N \times 1024}$ and neck $e_{\text{neck}} \in \mathbb{R}^{N \times 1024}$ features to obtain $e_{\text{final}} \in \mathbb{R}^{N \times 1024}$ as the cross-attention guide for the UNet.

3.1.1 Glyph Transformer

The intention of designing the Glyph Transformer is that we can use cross-attention to capture the interaction between character-level local features and line-level global features to get a better representation of text glyphs. This is inspired by Cutie Cheng et al. [2023], a video segmentation work that used a cross-attention mechanism to capture relationships between local features at the pixel level and global features at the object level and eventually achieved state-of-the-art results in various video segmentation metrics and test datasets.

Figure 3 illustrates the details of our Glyph Transformer. Given the d_{local} and d_{global} features extracted by F_{OCR} , we first repeat $1 \times d_{\text{global}}$ to $N \times d_{\text{global}}$ to match the $N \times d_{\text{local}}$ local features. Then we project both of them to

the d_{model} size. Next, we transform these projected features through learned linear projections where local features generate queries (Q) and values (V), while global features produce keys (K). We then apply rotary positional embedding (ROPE) to Q and K, effectively computing: $Q', K' = \text{ROPE}(Q, K)$ where Q' and K' are the positionally-encoded versions of Q and K, respectively.

Experimentally, we found that without adding positional embedding, the generated text would have been disordered, meaning that characters would appear in random order. The choice of using ROPE instead of other positional embedding techniques is due to the fact that it integrates positional information after projection, avoiding the need to add embeddings twice for differently dimensioned local and global features. We then perform standard cross-attention. This mechanism enables the model to leverage global context to enhance the understanding of local features in relation to text glyphs. The resulting attended features, $e_{attended}$, are in the d_{model} dimension. Finally, we project these features to the desired output dimension d_{output} to obtain the final conditions.

3.1.2 Backbone Fusion Module

To produce enhanced e^{global} features, we designed a feature fusion module for the backbone, which is inspired by feature pyramid networks. This module can be generalized to various pretrained OCR recognition models, with our implementation specifically tailored for the PaddleOCR-V4 model.

In general, given a set of multiscale features x_1, x_2, \dots, x_N extracted from a backbone model, where $x_i \in \mathbb{R}^{C_i \times H_i \times W_i}$, our fusion module first projects each feature map to a common dimension D : $c_i = f_i(x_i)$, where $f_i: \mathbb{R}^{C_i \times H_i \times W_i} \rightarrow \mathbb{R}^{D \times H_i \times W_i}$. The features are then fused in a top-down manner, starting with $p_N = c_N$, and for $i = N - 1, \dots, 1$: $p_i = g_i(u(p_{i+1}) + c_i)$. Finally, the output is generated as $y = h(d(k(p_1)))$. Here, $u(\cdot)$ represents upsampling, g_i are fusion operations, k is a final projection, d is downsampling, and h is a pooling operation.

For our specific implementation with the PaddleOCR-V4 model, we use five levels of features x_1, x_2, x_3, x_4, x_5 , where $x_i \in \mathbb{R}^{C_i \times H_i \times W_i}$. We apply 1x1 convolutions for the lateral connections: $c_i = f_i(x_i)$, where $f_i: \mathbb{R}^{C_i \times H_i \times W_i} \rightarrow \mathbb{R}^{D \times H_i \times W_i}$. Starting from the top level, we have $p_5 = c_5$, and for $i = 4, 3, 2, 1$: $p_i = g_i(u(p_{i+1}) + c_i)$, where g_i is a 3x3 convolution. The final output is obtained by $y = h(d(k(p_1)))$, where k is a 1x1 convolution, d is downsampling, and h is adaptive average pooling.

This model design adapts easily to various pretrained OCR recognition models while improving the quality of e^{global} features. Our Backbone Fusion Module leverages multi-level feature maps to capture fine-grained representations of text characters, potentially enhancing text recognition accuracy. In our ablation studies, we observed clear improvements in the model’s text generation performance, demonstrating the module’s effectiveness.

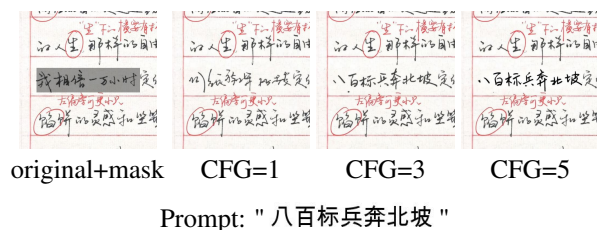


Figure 4: Effect of classifier-free guidance (CFG). Original image with target area mask shown leftmost. Without CFG (CFG=1), TextMastero produces unreadable text. CFG=3 improves readability while maintaining style. CFG=5 generates overly thick text, deviating from the original region.

3.1.3 Classifier-Free Guidance

Classifier-free guidance (CFG) has been shown to be effective in controlling the strength of prompt-following ability in text-to-image LDMs Rombach et al. [2022]. Hence, we train our scene text editing model with a certain probability of null glyph condition to leverage the CFG strength. Our experiments with CFG reveal a crucial trade-off in scene text editing. As demonstrated in Figure 4, we found that in inference, a higher CFG scale results in stronger glyph control, producing clearer and thicker text. This allows for improved readability when editing texts. However, our findings show that this comes at a cost to style preservation. Conversely, lower CFG scales excel at maintaining the original text style, though occasionally at the expense of target text accuracy. This insight offers a new approach to balancing readability and style preservation in scene text editing tasks.

| Model | Text Accuracy | | | | Style Similarity | | | |
|---------|--------------------|---------------|------------------|---------------|------------------|----------------|------------------------|---------------|
| | Sen.Acc \uparrow | | CER \downarrow | | FID \downarrow | | Avg.LPIPS \downarrow | |
| | English | Chinese | English | Chinese | English | Chinese | English | Chinese |
| DiffUTE | 0.3319 | 0.2523 | 0.3186 | 0.4048 | 14.3176 | 24.9295 | 0.1313 | 0.2056 |
| AnyText | 0.6067 | 0.5801 | 0.1730 | 0.2088 | 10.4257 | 24.9004 | 0.1098 | 0.1978 |
| Ours | 0.8170 | 0.7301 | 0.0741 | 0.1341 | 4.6101 | 11.8915 | 0.0545 | 0.1007 |

Table 1: Model comparison results.

3.2 Latent Guidance Module

The latent guidance module mainly controls the visual appearance of the generated text (i.e., style control). Figure 2 (bottom) demonstrates our latent guidance module. The first three inputs, x, m, x_m , are the standard in-painting formulation proposed by Rombach et al. [2022], where x and x_m are encoded by VAE to become latent $4 \times H/8 \times W/8$, and the mask m is interpolated to $1 \times H/8 \times W/8$. Together, they form a 9-channel input feature map for UNet $z_t^{inpaint}$. Then it is fed into the input convolution of the UNet to produce $y_t^{inpaint}$. In addition to that, we introduce a convolutional style encoder E_{style} to capture the nuances of the style from the masked region c_{style} , as a time-independent latent feature y^{glyph} . Following Zhang et al. [2023], we use zero convolution improve representation quality. It reads:

$$y^{style} = ZeroModule(E_{style}(c_{style})) \quad (1)$$

Finally, we concatenate $y_t^{inpaint}$, and y^{style} and use another convolution layer to match the UNet’s original input dimensions. That is,

$$z_t = Conv(Concat(y_t^{inpaint}, y^{style})) \quad (2)$$

This design effectively encapsulates position information, glyph style, and style nuances at the same time.

4 Experiments

4.1 Dataset

We use AnyWord-3M Tuo et al. [2024], a dataset for scene text generation and scene text editing, as our training set. We utilize the dataset specifically for scene text editing scenario: each sample is an image containing multiple line-level annotations, which consists of text content, and its corresponding polygonal position as target area to generate new text. Since each image can have multiple text regions, we randomly sample one text-position pair in training. Our dataset formulation can be written as:

$$\mathcal{D} = \{(I_i, \{(T_{ij}, P_{ij})\}_{j=1}^{M_i})\}_{i=1}^N$$

N is the total number of images, approximately 3.5 million in case of AnyWord dataset. M is number of text-position pairs in the i th image. Hence (T_{ij}, P_{ij}) would be a single data sample.

4.2 Implementation Details

We initialize our VAE and UNet with stable-diffusion 2.1 weights Rombach et al. [2022]. Each glyph Transformer has four layers and two heads, and $d_{output} = 1024$ to match with UNet’s conditional embedding dimension; their weights are initialized randomly. Latent guidance module’s style encoder is a two-layer convolutional module mapping style image $c_{style} \in \mathbb{R}^{3 \times 128 \times 128}$ to $y_{style} \in \mathbb{R}^{128 \times 64 \times 64}$, to allow concatenation with $y_t^{inpaint} \in \mathbb{R}^{320 \times 64 \times 64}$, resulting $\mathbb{R}^{448 \times 64 \times 64}$ intermediate latents. Finally, a zero-convolution layer is used to map $\mathbb{R}^{448 \times 64 \times 64}$ back to $\mathbb{R}^{320 \times 64 \times 64}$. That gives us the final style-guided latent z_t . Cross attention condition e_{final} and latent guidance z_t are then used to train the UNet. Our model was trained for 15 epochs with a global batch size of 256 on 8 V100S-32G cards. We also use a null condition probability of 0.1 to allow classifier free guidance in inference.

4.3 Comparisons

4.3.1 Setup

We evaluate our model using AnyText-Eval Tuo et al. [2024] for quantitative analysis (2000 images, 4181 English and 2092 Chinese text-position pairs) and a curated dataset of 80 challenging stylistic images (120 text-position pairs) for qualitative assessment. While AnyText-Eval provides statistical coverage, its target texts match the original, not fully



Figure 5: Comparison of scent text editing methods: DiffUTE, AnyText, and our *TextMastero*. More results are available in supplementary materials.

reflecting real-world editing tasks. Our curated dataset focuses on challenging stylistic variations and incorporates new text contents.

We benchmark against state-of-the-art models DiffUTE Chen et al. [2023a] and AnyText. For AnyText, we use the public AnyWord-3M checkpoint. We trained DiffUTE on AnyWord-3M for 15 epochs with a batch size of 256 and null condition probability of 0.1, matching our model’s hyperparameters. All methods use DDIM Song et al. [2021] sampler with 20 steps denoising steps during inference, with CFG scale 9 for AnyText and 3 for ours and DiffUTE.

While other diffusion-based scene text editing methods exist (e.g., TextDiffuser Chen et al. [2023b], GlyphDraw Ma et al. [2023], and GlyphControl Yang et al. [2023]), we focus on DiffUTE and AnyText for two reasons: they are multilingual, aligning with our emphasis on multilingual scene text editing, and AnyText has demonstrated significant superiority over these alternatives in comprehensive evaluations. This approach ensures our comparison is against the most advanced methods in the field.

| Ablation Setting | Text Accuracy | | | | Style Similarity | | | |
|--|---------------|---------------|---------------|---------------|------------------|----------------|---------------|---------------|
| | Sen.Acc ↑ | | CER ↓ | | FID ↓ | | Avg.LPIPS ↓ | |
| | English | Chinese | English | Chinese | English | Chinese | English | Chinese |
| <i>Glyph Conditioning Module</i> | | | | | | | | |
| Full model | 0.5494 | 0.5120 | 0.1766 | 0.2367 | 30.9095 | 51.3762 | 0.1190 | 0.2134 |
| w/o multi-level fusion | 0.4536 | 0.3698 | 0.2470 | 0.3314 | 32.4550 | 53.0127 | 0.1247 | 0.2208 |
| w/o backbone feature (1 glyph TFM) | 0.5065 | 0.4271 | 0.2128 | 0.2987 | 30.5866 | 49.6588 | 0.1196 | 0.2110 |
| w/o neck cross attention (0 glyph TFM) | 0.3263 | 0.2735 | 0.3137 | 0.3916 | 30.6271 | 51.6288 | 0.1211 | 0.2121 |
| <i>Latent Guidance Module</i> | | | | | | | | |
| Full model | 0.5494 | 0.5120 | 0.1766 | 0.2367 | 30.9095 | 51.3762 | 0.1190 | 0.2134 |
| w/o style encoder | 0.5150 | 0.5015 | 0.1925 | 0.2465 | 35.8388 | 53.0539 | 0.1405 | 0.2229 |

Table 2: Ablation study results.

4.3.2 Quantitative

We measure four metrics for quantitative studies: sentence accuracy (Sen.Acc) and character error rate (CER) for text content fidelity; Fréchet Inception Distance (FID)Seitzer [2020] and LPIPS Zhang et al. [2018] for style similarity. Sen.Acc measures line-level accuracy, while CER is for character-level accuracy. FID measures distribution-level style similarity, while LPIPS focuses on sample-level similarity. We average LPIPS distances over all samples for the final measurement. FID and LPIPS are measured between cropped ground truth image and generated text regions, as scene text editing aims to maintain similarity in the edited region while leaving non-target regions unchanged.

Table 1 shows our method significantly outperforms prior arts in both text generation accuracy and style similarity. Our overall sentence accuracy (averaging English and Chinese results) is 48.14% and 18.02% higher than DiffUTE and AnyText, respectively; CER is 25.76% and 8.68% lower. Note that the evaluation OCR predictor ModelScope [2023] often fails to recognize stylish characters our model generates correctly, suggesting actual accuracy may be higher than reported. Our method also better maintains style similarity, with substantially lower FID and LPIPS distances compared to DiffUTE and AnyText.

4.3.3 Qualitative

Figure 5 shows some comparison results among our method, AnyText, and DiffUTE. Our method is substantially better than prior arts on both text accuracy and style similarity. More qualitative results are available in the supplementary materials.

4.4 Ablations

We evaluate each component’s effectiveness by ablating them sequentially. For the glyph conditioning module, we first remove multi-level fusion, then backbone features entirely (eliminating one glyph transformer), and finally both glyph transformers, resulting in a vanilla structure using only character-level glyph images to extract $N \times 720$ features. We add absolute positional embeddings and project them to $N \times 1024$ to be compatible with SD2.1’s UNet. For the latent guidance module, we ablate our style encoder. All experiments used a 375K image subset of Anyword-3M, trained for 15 epochs with a batch size of 256 on 4 A100-40G cards.

Table 2 shows quantitative results. Without multi-level fusion, we see an 11.9% average sentence accuracy drop for English and Chinese texts. Removing backbone features and one glyph transformer results in a 6.39% drop, performing better than using only the last hidden states of OCR backbone. This suggests that backbone and neck features have distinct distributions, which our FPN-like fusion module addresses by introducing parameters for multi-level feature fusion. The vanilla module shows a 23.08% sentence accuracy drop. CER results verify these trends.

Style similarity remains consistent across glyph conditioning ablations, as expected since these primarily affect text accuracy. For the latent guidance module, average FID for English and Chinese generations increases by 3.3035, and average Avg.LPIPS by 0.0845, indicating our style encoder’s role in maintaining style similarity post-editing.

5 Conclusion & Future Works

We introduced TextMastero, a novel framework for multilingual scene text editing based on latent diffusion models. Our approach addresses challenges in generating complex glyphs, particularly CJK characters, in stylistic scenes. Key innovations include a glyph conditioning module for fine-grained content control and a latent guidance module for style consistency. Experiments demonstrate TextMastero’s superior performance in text fidelity and style similarity across diverse languages and visual scenarios. Future work could enhance style similarity and generation stability using networks like VGG Simonyan and Zisserman [2015] for style feature extraction, and expand support to more minority languages beyond CJK to increase impact and accessibility.

References

- Junyeop Lee, Yoonsik Kim, Seonghyeon Kim, Moonbin Yim, Seung Shin, Gayoung Lee, and Sungrae Park. Rewritten: Realistic scene text image generation via editing text in real-world image. *CoRR*, abs/2107.11041, 2021. URL <https://arxiv.org/abs/2107.11041>.
- Liang Wu, Chengquan Zhang, Jiaming Liu, Junyu Han, Jingtuo Liu, Errui Ding, and Xiang Bai. Editing text in the wild. In Laurent Amsaleg, Benoit Huet, Martha A. Larson, Guillaume Gravier, Hayley Hung, Chong-Wah Ngo, and Wei Tsang Ooi, editors, *Proceedings of the 27th ACM International Conference on Multimedia, MM 2019, Nice, France, October 21-25, 2019*, pages 1500–1508. ACM, 2019. doi:10.1145/3343031.3350929. URL <https://doi.org/10.1145/3343031.3350929>.
- Prasun Roy, Saumik Bhattacharya, Subhankar Ghosh, and Umapada Pal. STEFANN: scene text editor using font adaptive neural network. In *2020 IEEE/CVF Conference on Computer Vision and Pattern Recognition, CVPR 2020, Seattle, WA, USA, June 13-19, 2020*, pages 13225–13234. Computer Vision Foundation / IEEE, 2020. doi:10.1109/CVPR42600.2020.01324. URL https://openaccess.thecvf.com/content_CVPR_2020/html/Roy_STEFANN_Scene_Text_Editor_Using_Font_Adaptive_Neural_Network_CVPR_2020_paper.html.
- Yadong Qu, Qingfeng Tan, Hongtao Xie, Jianjun Xu, YuXin Wang, and Yongdong Zhang. Exploring stroke-level modifications for scene text editing. In Brian Williams, Yiling Chen, and Jennifer Neville, editors, *Thirty-Seventh AAAI Conference on Artificial Intelligence, AAAI 2023, Thirty-Fifth Conference on Innovative Applications of Artificial Intelligence, IAAI 2023, Thirteenth Symposium on Educational Advances in Artificial Intelligence, EAAI 2023, Washington, DC, USA, February 7-14, 2023*, pages 2119–2127. AAAI Press, 2023. doi:10.1609/AAAI.V37I2.25305. URL <https://doi.org/10.1609/aaai.v37i2.25305>.
- Jonathan Ho, Ajay Jain, and Pieter Abbeel. Denoising diffusion probabilistic models. In Hugo Larochelle, Marc’Aurelio Ranzato, Raia Hadsell, Maria-Florina Balcan, and Hsuan-Tien Lin, editors, *Advances in Neural Information Processing Systems 33: Annual Conference on Neural Information Processing Systems 2020, NeurIPS 2020, December 6-12, 2020, virtual*, 2020. URL <https://proceedings.neurips.cc/paper/2020/hash/4c5bcfec8584af0d967f1ab10179ca4b-Abstract.html>.
- Jiabao Ji, Guanhua Zhang, Zhaowen Wang, Bairu Hou, Zhifei Zhang, Brian Price, and Shiyu Chang. Improving diffusion models for scene text editing with dual encoders. *CoRR*, abs/2304.05568, 2023. doi:10.48550/ARXIV.2304.05568. URL <https://doi.org/10.48550/arXiv.2304.05568>.
- Haoxing Chen, Zhuoer Xu, Zhangxuan Gu, Jun Lan, Xing Zheng, Yaohui Li, Changhua Meng, Huijia Zhu, and Weiqiang Wang. Diffute: Universal text editing diffusion model. In Alice Oh, Tristan Naumann, Amir Globerson, Kate Saenko, Moritz Hardt, and Sergey Levine, editors, *Advances in Neural Information Processing Systems 36: Annual Conference on Neural Information Processing Systems 2023, NeurIPS 2023, New Orleans, LA, USA, December 10 - 16, 2023*, 2023a. URL http://papers.nips.cc/paper_files/paper/2023/hash/c7138635035501eb71b0adf6ddc319d6-Abstract-Conference.html.

- Yuxiang Tuo, Wangmeng Xiang, Jun-Yan He, Yifeng Geng, and Xuansong Xie. Anytext: Multilingual visual text generation and editing. In *The Twelfth International Conference on Learning Representations, ICLR 2024, Vienna, Austria, May 7-11, 2024*. OpenReview.net, 2024. URL <https://openreview.net/forum?id=ezBH9WE9s2>.
- Yuxiang Tuo, Wangmeng Xiang, Jun-Yan He, Yifeng Geng, and Xuansong Xie. Anytext: Multilingual visual text generation and editing. *CoRR*, abs/2311.03054, 2023. doi:10.48550/ARXIV.2311.03054. URL <https://doi.org/10.48550/arXiv.2311.03054>.
- Minghao Li, Tengchao Lv, Jingye Chen, Lei Cui, Yijuan Lu, Dinei A. F. Florêncio, Cha Zhang, Zhoujun Li, and Furu Wei. Trocr: Transformer-based optical character recognition with pre-trained models. In Brian Williams, Yiling Chen, and Jennifer Neville, editors, *Thirty-Seventh AAAI Conference on Artificial Intelligence, AAAI 2023, Thirty-Fifth Conference on Innovative Applications of Artificial Intelligence, IAAI 2023, Thirteenth Symposium on Educational Advances in Artificial Intelligence, EAAI 2023, Washington, DC, USA, February 7-14, 2023*, pages 13094–13102. AAAI Press, 2023. doi:10.1609/AAAI.V37I11.26538. URL <https://doi.org/10.1609/aaai.v37i11.26538>.
- Lvmin Zhang, Anyi Rao, and Maneesh Agrawala. Adding conditional control to text-to-image diffusion models. In *IEEE/CVF International Conference on Computer Vision, ICCV 2023, Paris, France, October 1-6, 2023*, pages 3813–3824. IEEE, 2023. doi:10.1109/ICCV51070.2023.00355. URL <https://doi.org/10.1109/ICCV51070.2023.00355>.
- Chitwan Saharia, William Chan, Saurabh Saxena, Lala Li, Jay Whang, Emily L. Denton, Seyed Kamyar Seyed Ghasemipour, Raphael Gontijo Lopes, Burcu Karagol Ayan, Tim Salimans, Jonathan Ho, David J. Fleet, and Mohammad Norouzi. Photorealistic text-to-image diffusion models with deep language understanding. In Sanmi Koyejo, S. Mohamed, A. Agarwal, Danielle Belgrave, K. Cho, and A. Oh, editors, *Advances in Neural Information Processing Systems 35: Annual Conference on Neural Information Processing Systems 2022, NeurIPS 2022, New Orleans, LA, USA, November 28 - December 9, 2022*, 2022. URL http://papers.nips.cc/paper_files/paper/2022/hash/ec795aeadae0b7d230fa35cbaf04c041-Abstract-Conference.html.
- Robin Rombach, Andreas Blattmann, Dominik Lorenz, Patrick Esser, and Björn Ommer. High-resolution image synthesis with latent diffusion models. In *IEEE/CVF Conference on Computer Vision and Pattern Recognition, CVPR 2022, New Orleans, LA, USA, June 18-24, 2022*, pages 10674–10685. IEEE, 2022. doi:10.1109/CVPR52688.2022.01042. URL <https://doi.org/10.1109/CVPR52688.2022.01042>.
- Olaf Ronneberger, Philipp Fischer, and Thomas Brox. U-net: Convolutional networks for biomedical image segmentation. In Nassir Navab, Joachim Hornegger, William M. Wells III, and Alejandro F. Frangi, editors, *Medical Image Computing and Computer-Assisted Intervention - MICCAI 2015 - 18th International Conference Munich, Germany, October 5 - 9, 2015, Proceedings, Part III*, volume 9351 of *Lecture Notes in Computer Science*, pages 234–241. Springer, 2015. doi:10.1007/978-3-319-24574-4_28. URL https://doi.org/10.1007/978-3-319-24574-4_28.
- Kaiming He, Xiangyu Zhang, Shaoqing Ren, and Jian Sun. Deep residual learning for image recognition. In *2016 IEEE Conference on Computer Vision and Pattern Recognition, CVPR 2016, Las Vegas, NV, USA, June 27-30, 2016*, pages 770–778. IEEE Computer Society, 2016. doi:10.1109/CVPR.2016.90. URL <https://doi.org/10.1109/CVPR.2016.90>.
- Tsung-Yi Lin, Piotr Dollár, Ross B. Girshick, Kaiming He, Bharath Hariharan, and Serge J. Belongie. Feature pyramid networks for object detection. In *2017 IEEE Conference on Computer Vision and Pattern Recognition, CVPR 2017, Honolulu, HI, USA, July 21-26, 2017*, pages 936–944. IEEE Computer Society, 2017. doi:10.1109/CVPR.2017.106. URL <https://doi.org/10.1109/CVPR.2017.106>.
- Dongsheng Jiang, Yuchen Liu, Songlin Liu, Jin’e Zhao, Hao Zhang, Zhen Gao, Xiaopeng Zhang, Jin Li, and Hongkai Xiong. From clip to dino: Visual encoders shout in multi-modal large language models, 2024. URL <https://arxiv.org/abs/2310.08825>.
- Alec Radford, Jong Wook Kim, Chris Hallacy, Aditya Ramesh, Gabriel Goh, Sandhini Agarwal, Girish Sastry, Amanda Askell, Pamela Mishkin, Jack Clark, Gretchen Krueger, and Ilya Sutskever. Learning transferable visual models from natural language supervision. In Marina Meila and Tong Zhang, editors, *Proceedings of the 38th International Conference on Machine Learning, ICML 2021, 18-24 July 2021, Virtual Event*, volume 139 of *Proceedings of Machine Learning Research*, pages 8748–8763. PMLR, 2021. URL <http://proceedings.mlr.press/v139/radford21a.html>.
- Maxime Oquab, Timothée Darcet, Théo Moutakanni, Huy Vo, Marc Szafraniec, Vasil Khalidov, Pierre Fernandez, Daniel Haziza, Francisco Massa, Alaaeldin El-Nouby, Mahmoud Assran, Nicolas Ballas, Wojciech Galuba, Russell Howes, Po-Yao Huang, Shang-Wen Li, Ishan Misra, Michael G. Rabbat, Vasu Sharma, Gabriel Synnaeve, Hu Xu, Hervé Jégou, Julien Mairal, Patrick Labatut, Armand Joulin, and Piotr Bojanowski. Dinov2: Learning robust visual features without supervision. *CoRR*, abs/2304.07193, 2023. doi:10.48550/ARXIV.2304.07193. URL <https://doi.org/10.48550/arXiv.2304.07193>.

- PaddlePaddle. PP-OCRv4. https://github.com/PaddlePaddle/PaddleOCR/blob/release/2.7/doc/doc_ch/PP-OCRv4_introduction.md, 2023. Accessed: 2024-07-31.
- Ho Kei Cheng, Seoung Wug Oh, Brian Price, Joon-Young Lee, and Alexander G. Schwing. Putting the object back into video object segmentation. *CoRR*, abs/2310.12982, 2023. doi:10.48550/ARXIV.2310.12982. URL <https://doi.org/10.48550/arXiv.2310.12982>.
- Jiaming Song, Chenlin Meng, and Stefano Ermon. Denoising diffusion implicit models. In *9th International Conference on Learning Representations, ICLR 2021, Virtual Event, Austria, May 3-7, 2021*. OpenReview.net, 2021. URL <https://openreview.net/forum?id=St1giarCHLP>.
- Jingye Chen, Yupan Huang, Tengchao Lv, Lei Cui, Qifeng Chen, and Furu Wei. Textdiffuser: Diffusion models as text painters. In Alice Oh, Tristan Naumann, Amir Globerson, Kate Saenko, Moritz Hardt, and Sergey Levine, editors, *Advances in Neural Information Processing Systems 36: Annual Conference on Neural Information Processing Systems 2023, NeurIPS 2023, New Orleans, LA, USA, December 10 - 16, 2023*, 2023b. URL http://papers.nips.cc/paper_files/paper/2023/hash/1df4afb0b4ebf492a41218ce16b6d8df-Abstract-Conference.html.
- Jian Ma, Mingjun Zhao, Chen Chen, Ruichen Wang, Di Niu, Haonan Lu, and Xiaodong Lin. Glyphdraw: Learning to draw chinese characters in image synthesis models coherently. *CoRR*, abs/2303.17870, 2023. doi:10.48550/ARXIV.2303.17870. URL <https://doi.org/10.48550/arXiv.2303.17870>.
- Yukang Yang, Dongnan Gui, Yuhui Yuan, Weicong Liang, Haisong Ding, Han Hu, and Kai Chen. Glyphcontrol: Glyph conditional control for visual text generation. In Alice Oh, Tristan Naumann, Amir Globerson, Kate Saenko, Moritz Hardt, and Sergey Levine, editors, *Advances in Neural Information Processing Systems 36: Annual Conference on Neural Information Processing Systems 2023, NeurIPS 2023, New Orleans, LA, USA, December 10 - 16, 2023*, 2023. URL http://papers.nips.cc/paper_files/paper/2023/hash/8951bbdcf234132bcce680825e7cb354-Abstract-Conference.html.
- Maximilian Seitzer. pytorch-fid: FID Score for PyTorch. <https://github.com/mseitzer/pytorch-fid>, August 2020. Version 0.3.0.
- Richard Zhang, Phillip Isola, Alexei A Efros, Eli Shechtman, and Oliver Wang. The unreasonable effectiveness of deep features as a perceptual metric. In *CVPR*, 2018.
- ModelScope. Duguangocr. https://modelscope.cn/models/damo/cv_convnextTiny_ocr-recognition-general_damo/summary, 2023. Accessed: 2023.
- Karen Simonyan and Andrew Zisserman. Very deep convolutional networks for large-scale image recognition. In Yoshua Bengio and Yann LeCun, editors, *3rd International Conference on Learning Representations, ICLR 2015, San Diego, CA, USA, May 7-9, 2015, Conference Track Proceedings*, 2015. URL <http://arxiv.org/abs/1409.1556>.